

Generation of active Co(III) and peroxodiphosphate by synergistic electrocatalytic system with phosphate and the mediator cobalt(II) and its degradation performance

Dongmei Li, Wenjie Li, Quan Zhang, Yizhi Wang, Hongyu Lin, Li Feng, Shaoxiu Li, Yue Deng, Qiurong Xiao, Jiongxi Chen and Qi Dong

ABSTRACT

The promising synergistic electrocatalytic system of phosphate (PO_4^{3-}) with the mediator cobalt(II) (for short E-Co(II)- PO_4^{3-}) was employed to degrade cationic dye methylene blue (MB). The exploration in the electrocatalytic process revealed that the main intermediate active oxidation products were Co(III), accompanied with hydroxyl radicals and peroxodiphosphates ($\text{P}_2\text{O}_8^{4-}$). Their synergistic electrocatalytic degradation rate to MB and total organic carbon (TOC) was up to 100 and 60% in 40 min, respectively, which was 5 times and 2.6 times that in a direct electrocatalytic system, correspondingly. The degradation process of the E-Co(II)- PO_4^{3-} system on MB started with the bond being broken at the N-C junction of the MB molecule and intermediate active oxidation substances being generated, such as phenothiazine, 2-amino-5-(N-methylformamide) benzene sulfonic acid and N_1, N_1 -dimethyl-1,4 diaminobenzene. Then, the intermediates were degraded into aniline, phenol and benzene sulfonic acid, and eventually decomposed into inorganic substances like CO_2 and water. The electrocatalytic degradation mechanism of E-Co(II)- PO_4^{3-} system on MB was the combination of indirect oxidation of the intermediate oxidants like Co(III), $\text{P}_2\text{O}_8^{4-}$ and the hydroxyl radical with direct electrocatalysis on the platinum titanium electrode, where the electrocatalytic oxidation of Co(III) was dominant.

Key words | cationic dye wastewater, degradation performance, E-Co (II)- PO_4^{3-} electrocatalytic reaction system, electrocatalytic oxidation mechanism, optimal reaction conditions

HIGHLIGHTS

- Active Co(III) and peroxodiphosphate generated in a novel electrocatalytic system have synergistic electrocatalytic effect.
- MB removal rate reached 100% in 40 min in the novel electrocatalytic system with phosphate and the mediator cobalt(II).
- Co(III) is the dominant active oxidation substance in MB oxidation and mineralization.

Dongmei Li (corresponding author)

Wenjie Li

Quan Zhang

Li Feng

Shaoxiu Li

Qiurong Xiao

Jiongxi Chen

Qi Dong

Faculty of Civil and Transportation Engineering,
Guangdong University of Technology,
100 Waihuan Road West, HEMC,
Guangzhou 510006,
China

E-mail: ldm108@gdut.edu.cn;

ldm108@163.com

Yizhi Wang

Department of Brain and Cognitive Science,
Massachusetts Institute of Technology,
77 Massachusetts Avenue, Cambridge,
MA 02139,
USA

Hongyu Lin

Concord Academy,
166 Main Street,
Concord,
MA 01742,
USA

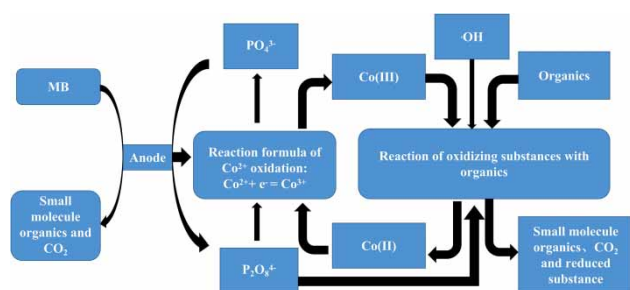
Yue Deng

Experimental School affiliated to Zhuhai No.1
Middle School,
393 Road 3rd Gongbei Gang,
Zhuhai 519000,
China

This is an Open Access article distributed under the terms of the Creative Commons Attribution Licence (CC BY 4.0), which permits copying, adaptation and redistribution, provided the original work is properly cited (<http://creativecommons.org/licenses/by/4.0/>).

doi: 10.2166/wst.2021.017

GRAPHICAL ABSTRACT



INTRODUCTION

Most of the organic pollutants (especially colored dye pollutants) in industrial wastewater are difficult to degrade, and it is hard to meet the standards through conventional treatment processes or their enhancement (Brillas 2020). Colored dyes are mutagenic, carcinogenic, and allergic (Dassanayake *et al.* 2018). Studies have shown that even wastewater containing only small amounts of dyes could seriously affect the growth of aquatic organisms (Sekar *et al.* 2012). Among them, most dyeing industries prefer to use cationic dyes. However, cationic dyes are more toxic than anionic dyes because of their aromatic ring structure of delocalized electron and special synthetic methods (Doltabadi *et al.* 2016). Therefore, how to efficiently degrade cationic dyes (such as rhodamine B (RhB), methylene violet (MV) and methylene blue (MB)) with low cost and high efficiency in industrial wastewater has become a challengeable issue (Cui *et al.* 2015).

There are several methods for the treatment of dye wastewater: ion exchange, flocculating sedimentation (Doltabadi *et al.* 2016), advanced oxidation technology (Dassanayake *et al.* 2018; Nidheesh *et al.* 2018), activated carbon adsorption (Doltabadi *et al.* 2016), and biodegradation (Dhall *et al.* 2012). Some of these physical technologies (such as activated carbon adsorption and flocculating sedimentation) have significant treatment efficacies, but they only transfer organic dyes from the liquid phase to solid for separation, which cause serious secondary pollution. The biological treatment method is not ideal for the treatment of dye wastewater, which has certain toxicity and is difficult to degrade. Advanced oxidation technology has drawn wide attention because some strong oxidizing active groups (such as hydroxyl radicals, sulfate radicals, etc) can oxidize and decompose organic pollutants to generate small molecules such as water and carbon dioxide

(Nidheesh *et al.* 2018). Among them, the ozonation and Fenton methods have significant effects on the degradation of pollutants. However, they require continuously adding oxidants to the wastewater, which increases the treatment cost. At the same time, a large amount of sludge is produced in the Fenton oxidation process; the initial investment in ozonation is large and more undegradable substances may be generated during the degradation process (Wang *et al.* 2019). Although photocatalytic technologies possess great advantages in energy utilization, the chromaticity of dye wastewater is large, which prevents the light source entering; at the same time, ultraviolet photocatalytic energy consumption is huge. Visible light catalytic efficiency is low, which is hardly satisfied in engineering application (Dassanayake *et al.* 2018). All these have limited the application of photocatalytic technology in the field of printing and dyeing wastewater treatment.

Nowadays, electrochemical technologies have been increasingly used in the treatment of wastewater containing refractory organics because of their high degradation performance. Among these electrochemical technologies, electrocoagulation and electrochemical oxidation are commonly adopted. Electrocoagulation is a widely spread method that uses iron and aluminum electrodes to conduct the coagulation reaction and directly generate coagulants via anodic dissolution. Recent research has focused on enhancing the oxidation capabilities of iron-based electrocoagulation by adding different oxidants; for example, adding potassium ferrate(VI) (Elnakar & Buchanan 2020). Iron-based electrocoagulation has the advantages of the abundance and low price of iron and easy operation, while its disadvantage is the high proportion of total iron dissolved under acid or neutral condition.

The electrochemical oxidation is one of the advanced oxidation technologies. There are noteworthy advantages

of electrocatalytic degradation on dyes, such as small space for the electrocatalytic device, low investment, easy operation with automation, wide application scope and high degradation efficiency. There are two types of electrocatalytic oxidation ways, direct oxidation and indirect. The direct electrochemical catalysis decomposes pollutants in water to achieve the degradation effect by anodic oxidation. In order to replace the expensive metal platinum electrode and boron doped diamond (BDD) electrode, with high electrochemical oxidation efficacy, the research in this area mainly focuses on electrode modification; for example, the modification of the titanium-based metal oxide electrode (Wang *et al.* 2013), carbon nanotube electrode (Yi *et al.* 2011) and three-dimensional electrode (Ghanbarlou *et al.* 2020). The issues for electrode modification mainly concern high oxidation efficiency, good stability, high oxygen evolution overpotential and low manufacturing cost. Indirect oxidation is also called mediated electrochemical oxidation (MEO), which is adopted to oxidize target pollutants by adding mediated ions in water. The main mechanism is that the mediated ions are oxidized at the anode to produce strongly oxidizing ions. In the process of oxidizing pollutants, the content of the mediated ions is not changed after redox (Govindan & Moon 2013) and favored by researchers (Chung & Park 2000; Costa *et al.* 2009; Soleymani & Moradi 2018). The common used mediated ions are silver ion (Ag^+), cerium ion (Ce^{3+}), cobalt ion (Co(II)), phosphate (PO_4^{3-}) and sulfate (SO_4^{2-}). Among them, the reaction of Ag^+ with chloride ions in water occurs easily and produces precipitates; Ce^{3+} owns lower solubility at normal pH; PO_4^{3-} and SO_4^{2-} react slowly with the electrodes. These ions are difficult to employ to establish an efficient electrochemical oxidation system. However, Co(II) is highly soluble in water, highly oxidizing, and reacts fast with electrodes (Chung & Park 2000). Therefore, the synergistic electrocatalysis reaction system with PO_4^{3-} and Co(II) was selected in this study.

Electrochemical oxidation is also called electrocatalysis because it only consumes electrical energy in the oxidation process. MEO can improve the energy utilization rate of direct electrocatalysis to a certain extent. Studies have shown that the MEO system could efficiently degrade a variety of refractory organic pollutants in strong acidic conditions (like concentrated sulfuric acid, concentrated nitric acid, and so on) (Lubis *et al.* 2015). However, the MEO system in conventional conditions has rarely been reported, which is not conducive for it to be popularized and put into use. Therefore, this study established a promising synergistic electrocatalysis reaction system with PO_4^{3-} and Co(II) (for

short $\text{E-Co(II)-PO}_4^{3-}$) and explored its oxidation mechanism and degradation performance.

MATERIALS AND METHODS

The calibration curve of methylene blue (MB) solution

MB standard solution was prepared at concentrations of 1 mg L^{-1} , 2 mg L^{-1} , 4 mg L^{-1} , 8 mg L^{-1} and 13 mg L^{-1} ; the corresponding absorbance at each concentration was measured at its maximum absorption wavelength (665 nm). Using the absorbance as the ordinate and the MB concentration as the abscissa, a calibration curve was depicted to clarify the linear equation of the correlation between the absorbance at 665 nm (noted as Y) and MB concentration (noted as X) for the solution is $Y = 0.1631X + 0.021$ with an R of 0.9993 (see Figure SI-1 in Supplementary Material).

Experimental materials and instruments

Experimental materials

Tert-butyl alcohol (TBA, $\text{C}_4\text{H}_{10}\text{O}$, molecular weight: 74) and cobalt sulfate ($\text{CoSO}_4 \cdot 7\text{H}_2\text{O}$, molecular weight: 281) were supplied by Tianjin Fuchen Chemical Reagent Co., Ltd. Methanol (CH_3OH , molecular weight: 32) was obtained from Tianjin Damao Chemical Reagent Factory. Methylene blue (MB, $\text{C}_{16}\text{H}_{18}\text{ClN}_3\text{S}$, molecular weight: 319.86) was provided by Tianjin Tianxin Fine Chemical Development Center. Platinum titanium electrode (width x height: $3.5 \text{ cm} \times 5 \text{ cm}$) was purchased from Suzhou Suntai Industrial Technology Co., Ltd, and 5,5-dimethyl-1-pyrroline-n-oxide (DMPO, $\text{C}_6\text{H}_{11}\text{NO}$, molecular weight: 113.16) from Aladdin. All the chemical reagents were of analytical grade.

Experimental equipment and procedures

Electrocatalysis experiment

The electrocatalysis experimental setup is shown in Figure 1. In the experiment, a stainless steel electrode clip was used to connect the cathode and anode, which were linked up to the direct current (DC) regulated power supply (MS305D, Maisheng Co., Ltd, 2018) by wire. The volume of the electrolytic cell was 700 mL, and the electrode interval was 2 cm. The experimental procedures are demonstrated below.

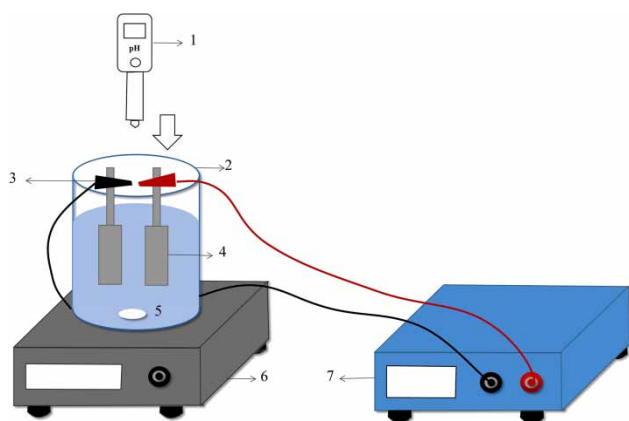


Figure 1 | The experimental setup of the electrocatalytic reactor. 1. pH meter 2. Cell (700 mL) 3. Electrode holders 4. Electrode plate (3.5 cm × 5 cm) 5. Magnetic rotor (800 r min⁻¹) 6. Magnetic stirrer (heating power: 150 W) 7. DC regulated power supply (voltage: 0–30 V; current: 0–5 A).

Firstly, the following experimental reagents were transferred to the electrolytic cell: 25 mM electrolyte sodium sulfate (Na₂SO₄), 2 mM cobalt sulfate, 3 mM sodium phosphate (Na₃PO₄) and 12.5 mg L⁻¹ MB solution (400 mL); the pH was adjusted to 4 with sulfuric acid (0.1 M) and sodium hydroxide (0.1 M) via pH meter (STARTER3100, OHAUS, USA, 2017), the magnetic stirrer (800 r min⁻¹, 79-1, Jintan Dadi Automation Instrument Factory, 2017) was started; the DC power supply was switched on and the current density adjusted to 12 mA cm⁻² to perform the electrocatalytic experiments.

During the electrocatalytic tests, the MB dye solution was sampled at the reaction time intervals of 5 min, 10 min, 15 min, 20, 30 and 40 min, and the absorbance of the corresponding sample measured; then the MB residual concentration (C_e) in the solution was obtained according to the calibrated standard curve shown in Figure SI-1. Thus, the degradation rate was achieved from the calculation $(1-C_e)/C_0$, where C_0 was the initial concentration of MB. The degradation performance at different electrocatalytic systems, like Co(II)-3 mM Na₂SO₄, E-3 mM Na₂SO₄, E-3 mM Na₂PO₄, E-Co(II), E-Co(II)-PO₄³⁻, were tested for obtaining an optimal electrocatalytic system. And then, the effect of different experimental factors on the optimal synergistic electrocatalysis efficacy were explored. The experimental factors were as follows: initial concentrations of Co(II) and PO₄³⁻, current density, initial pH, and electrolyte concentration. Each group of experiments was repeated three times, and the three experimental data were averaged to obtain the MB degradation rate.

Shielding experiment and capture test

There are some intermediate active oxidation substances existing in the liquid phase of the novel indirect

electrocatalytic system. The effect of the intermediate active oxidation products on MB can be masked by introducing a shielding agent into the system. The change of degradation rate can indirectly reveal the existence of intermediate products. In addition, based on the behaviors of the active oxygen species reacting with some capture agents producing complexes, the active oxygen species can be manifested by detecting the corresponding complex by introducing the matching capture agent into the system.

TBA and sodium thiosulfate (Na₂S₂O₃) were used for shielding experiments to screen the free radicals and all active oxidation substances in the solution. DMPO and ammonia were employed to capture free radicals and Co(III), respectively. Here, it should be noted that the concentration of the shielding agent should satisfy the condition that it would not affect the electrode direct electrocatalysis efficacy for MB.

RESULTS AND DISCUSSION

Types of intermediate oxidation products in E-Co(II)-PO₄³⁻ system

It was confirmed that the intermediate oxidation products, like free radicals and Co(III), existed in the E-Co(II)-PO₄³⁻ system by detecting the change of MB oxidation removal rate after introducing shielding agents such as TBA and Na₂S₂O₃ into the system. The results are shown in Figure 2.

Free radicals

TBA was introduced into the system for detecting hydroxyl radicals and sulfate radicals (Govindan & Moon 2013). As shown in Figure 2(a), after adding 40 mmol of TBA, the degradation efficiency of the system on MB decreased slightly (from 53% to 45% in 15 min), which indicated that a small amount of free radicals were generated during the degradation of MB in the E-Co(II)-PO₄³⁻ system. The degradation rate of MB was almost the same when the dosage of TBA increased to 100 mmol, which meant the oxidation ability of the free radicals in this electrocatalytic system was weak. With EPR spectrometer (EMXplus-10/12, Bruker, Germany, 2018) and DMPO as the capture agent, the type of free radicals were determined further. A weak hydroxyl radical atlas appeared in Figure 2(b), which proved the hydroxyl radical ($\cdot\text{OH}$) existed in the system.

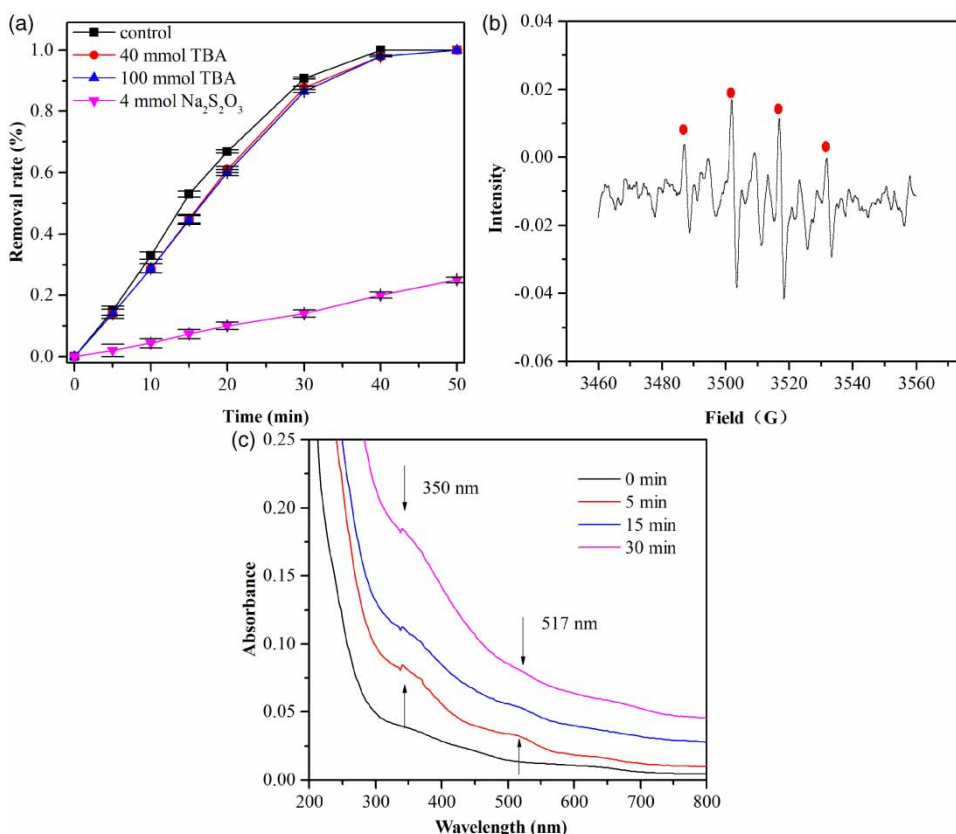


Figure 2 | (a) The effect of Na₂S₂O₃ and TBA on the removal rate of MB; (b) radicals EPR atlas; (c) detection of Co(III) by UV-vis spectra (reaction conditions: initial MB concentration = 12.5 mg L⁻¹; initial pH = 4; current = 12 mA cm⁻²; stirring speed = 800 r min⁻¹; [Co(III)] = 2 mM; [PO₄³⁻] = 3 mM; [Na₂SO₄] = 25 mM).

Determination of the strong intermediate oxidation products Co(III) and peroxodiphosphates (P₂O₈⁴⁻)

As a strong reducing agent, Na₂S₂O₃ is often used to detect the presence of oxidation substances in solution. By adding 4 mmol Na₂S₂O₃ to the E-Co(II)-PO₄³⁻ system, the degradation rate of the system on MB decreased significantly (from 100% to 20% in 40 min), which indirectly indicated that the electrocatalytic system produced intermediate products in the liquid phase that possessed a strong oxidative degradation effect on MB. It was concluded that the main intermediate oxidation product in the system was Co(III), and a small amount of hydroxyl radicals and P₂O₈⁴⁻ were also present, which was consistent with the results reported in the literature (Costa *et al.* 2009; Lubis *et al.* 2015).

The detection of Co(III)

Since the residence time of Co(III) at conventional pH is extremely short, it is difficult to measure directly. However, Co(III) can be captured by ammonia molecules to form a

variety of stable cobalt-amine complexes, which have the maximum absorption peak within the wavelength range of 320–520 nm (Okubo *et al.* 2010). The existence of Co(III) was verified with analysis on the characteristics of the solution by UV-Vis full-scan spectroscopy (UV-5100, Shanghai Yuanxi Instrument Co., Ltd, 2019) and introducing 25% of ammonia (1 mL) as the capture agent. The results shown in Figure 2(c) displayed that there were two absorption peaks at the wavelength 350 and 517 nm when the reaction time was at 5 min, 15 min, 30 min. These two absorption peaks revealed the existence of Co(III), which was consonant with the result reported by Okubo *et al.* (2010). As the reaction time went on, the amount of Co(III) has grown and more Co(III) was captured by the ammonia molecule, and the absorbance increased as well. The capture experiments confirmed the presence of Co(III).

The detection of P₂O₈⁴⁻

The P₂O₈⁴⁻ has a long residence time in solution, which was beneficial for detecting the presence of P₂O₈⁴⁻ by testing

whether MB kept decomposing after the E-Co(II)-PO₄³⁻ system was switched off. When the power was off for 10 min, the absorbance of the MB solution decreased from 1.400 to 1.393, which showed that P₂O₈⁴⁻ may present in the E-Co(II)-PO₄³⁻ system. However, the decrease of the absorbance was unobvious, which may be caused by the reaction between the P₂O₈⁴⁻ and Co(II), so that the P₂O₈⁴⁻ concentration in the system was decreased (Hariharan & Maruthamuthu 1979).

In order to eliminate the interference of sodium sulfate electrolyte, the electrolyte sodium phosphate was employed in the E-Co(II)-PO₄³⁻ system instead of sodium sulfate. KI-starch test paper was adopted to detect the presence of intermediate oxidation products in the reaction solution when the power was off. It was found that the KI-starch test paper was blue, which indicated that the oxidation substances still existed in the solution. Co(III) and hydroxyl radicals have extremely short residence time (Liu et al. 2018), which makes detecting their presence difficult. Hence, it was inferred that the intermediate oxidation product was P₂O₈⁴⁻.

Therefore, the main intermediate oxidation products existing in the E-Co(II)-PO₄³⁻ system were Co(III), and a small number of hydroxyl radicals and P₂O₈⁴⁻.

The comparison of degradation effects of several different catalytic systems on MB

The degradation effect of several different electrocatalytic systems on MB is shown in Figure 3. Under the condition of no electricity, when Co(II) and phosphate ions were acting on MB at the same time, the MB degradation did not happen within 50 min. After adding the electrolytes (25 mM Na₂SO₄ and 3 mM Na₃PO₄) with direct electrochemical

oxidation on MB by platinum plating on a titanium electrode for 30 min, the degradation rate was only 18%. In order to eliminate the influence of the Na₃PO₄ electrolyte, 3 mM Na₃PO₄ was replaced with 3 mM Na₂SO₄; then, the MB degradation rate was 20%. To take Na₂PO₄ as the electrolyte, the degradation efficiency of direct electrocatalysis was a bit higher than that by electrolyte Na₂SO₄. However, for the E-Co(II) system, the degradation rate of MB was up to 76.3% at 30 min. After the combination of the electrolytes PO₄³⁻ with the E-Co(II) system, the degradation rate grew to 91% within 30 min, and even reached 100% when the reaction time lengthened to 40 min. Therefore, in the process of MB degradation, the current utilization rate of direct electrochemical oxidation was low, and its degradation rate was less than 20%; however, the E-Co(II) system brought a much higher degradation rate (76.3%) and an improved current utilization rate compared with that of the direct electrochemical oxidation system. Furthermore, when the electrolyte Na₃PO₄ was coupled with E-Co(II) to form the E-Co(II)-PO₄³⁻ synergistic electrocatalytic system, the most exciting result was that the oxidative degradation rate on MB was up to 100% within 40 min, which was 5 times of that of the direct electrochemical oxidation system with electrolytes Na₂SO₄.

At the same time, the degree of mineralization of MB was explored by testing total organic carbon (TOC) residual concentration (measured by TOC analyzer, TOC-3000, Shanghai Yuanxi Instrument Co., Ltd, 2015) in the E-Co(II)-PO₄³⁻ electrocatalytic system and then compared with that in the direct electrocatalysis system (shown in Figure 3(b)). It was clearly shown that the TOC degradation rate reached 60% in the E-Co(II)-PO₄³⁻ system, 2.6 times that in the direct electrocatalysis system (23%) for 2.5 h, which demonstrated that the mineralization efficiency of the former was higher.

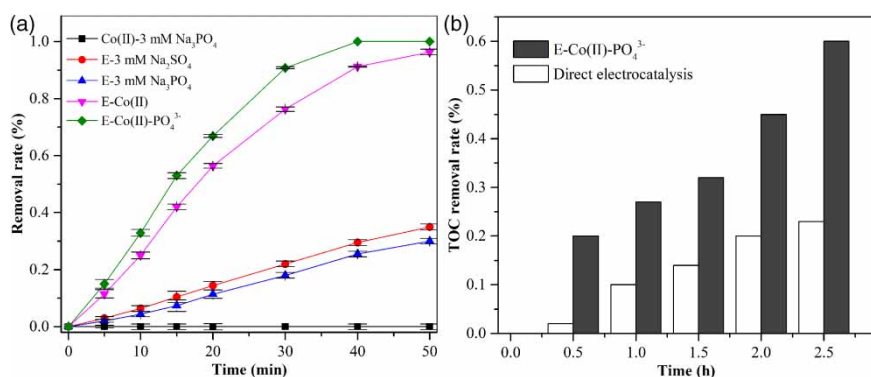


Figure 3 | (a) MB removal rate under different electrochemical systems; (b) TOC removal rate under E-Co(II)-PO₄³⁻ system and direct electrocatalytic system (reaction conditions: initial concentration = 12.5 mg L⁻¹; initial pH = 4; current = 12 mA cm⁻²; stirring speed = 800 r min⁻¹; [Co(III)] = 2 mM; [PO₄³⁻] = 3 mM; [Na₂SO₄] = 25 mM).

Comparison of degradation efficacy of E-Co(II)-PO₄³⁻ system on MB under different conditions

The electrocatalytic oxidation experiments of MB were conducted in the E-Co(II)-PO₄³⁻ system, and the influence of different factors below on the degradation efficacy of the system is presented in Figure 4(a)–4(e). The main influential factors were the concentration of Co(II), PO₄³⁻ and electrolyte, current density and initial pH.

Influence of initial Co(II) concentration

The effect of initial Co(II) concentration on the MB degradation of the E-Co(II)-PO₄³⁻ electrocatalytic system is shown in Figure 4(a).

From Figure 4(a), the oxidation ability of the E-Co(II)-PO₄³⁻ electrocatalytic system was enhanced significantly with the increase in Co(II) concentration. When the Co(II) concentration was set as 0 mM, 0.2 mM, 0.5 mM, 1, 2 and 4 mM, the MB degradation rate of the electrocatalytic system was 18%, 36%, 51%, 67%, 94% and 100% accordingly at 30 min. It was clear that the increasing of Co(II) concentration facilitated the yield per unit time of the strong oxidation substance -Co(III), which significantly enhanced the electrocatalytic performance of the E-Co(II)-PO₄³⁻ system (Lubis et al. 2015). At the same time, it could be seen that the degradation efficiency of this system was doubled at 0.2 mM of Co(II) compared to direct electrocatalysis. When the Co(II) concentration was up to 4 mM, the degradation efficacy of the E-Co(II)-PO₄³⁻ system was five times that of direct electrocatalysis. This phenomenon indicated that the cobalt ion dielectric system had an enhancing effect on the MB degradation rate and the current utilization efficiency.

Effect of initial PO₄³⁻ concentration

At different PO₄³⁻ concentrations, the degradation efficacy of the E-Co(II)-PO₄³⁻ system on MB is presented in Figure 4(b). When the concentration of PO₄³⁻ was 0 mM, 2 mM, 3 mM, 5, 8 and 10 mM, the degradation rate of E-Co(II)-PO₄³⁻ system for MB was 76.3%, 86.8%, 91%, 88.8%, 87.3% and 87.3%, respectively. The data showed that when the PO₄³⁻ concentration was lower (less than 3 mM), the oxidation ability of the system was improved remarkably with the increasing PO₄³⁻ concentration; however, when the PO₄³⁻ concentration was relatively higher (3 mM ~ 10 mM), the oxidation ability of the E-Co(II)-PO₄³⁻ system decreased slightly with the growing

concentration of PO₄³⁻. All these results were likely caused by the reactions happening in the E-Co(II)-PO₄³⁻ system; firstly, the amount of P₂O₈⁴⁻ augmented with the increase in PO₄³⁻ concentration; then P₂O₈⁴⁻ oxidized Co(II) to produce Co(III) (Hariharan & Maruthamuthu 1979), which enhanced the oxidation ability of the system. However, the increase in the PO₄³⁻ concentration caused the formation of more Co₃(PO₄)₂ precipitates on the cathode, which reduced the Co(II) in the liquid phase, leading to a decrease in the oxidation efficiency of the system. These two possible reasons resulted in a slight effect of the increasing PO₄³⁻ concentration on the oxidation efficiency of the E-Co(II)-PO₄³⁻ system.

Effect of initial pH value

The effect of initial pH value on the MB degradation efficacy of E-Co(II)-PO₄³⁻ system is shown in Figure 4(c). The degradation efficiency of the system increased gradually with the decrease in pH value. When the pH was 4, it reached the optimum electrocatalytic efficacy.

At the initial pH value 2, 4, 6, 7, 8 and 10, the electrocatalytic degradation rate on MB of the E-Co(II)-PO₄³⁻ system was 100%, 91%, 58%, 50%, 42% and 25% accordingly at 30 min. The results demonstrated that the degradation efficacy of the system gradually decreased with the growth in pH value. The main reason was that Co(II) existed in the form of Co(OH)₄²⁻ in alkaline solution, which reduced the oxidation performance of the system, while the acidic condition can inhibit side reactions (like the electrolysis of water) and the hydrolysis of Co(II). In addition, when the initial pH value was 4, 6, and 8, there were some black precipitates adhering to the cathode surface. This situation was even worse when pH was 6. In addition, the pH value of the cathode surface was higher than that of the solution in the electrocatalysis process, and a certain amount of Co(OH)_x and Co₃(PO₄)₂ precipitates were formed on the cathode surface (Chaplin 2014), which caused the decline in the degradation efficiency of the E-Co(II)-PO₄³⁻ system.

Effect of current density

Degradation efficacy of E-Co(II)-PO₄³⁻ system on MB at different current densities is shown in Figure 4(d). When the current density was set as 5 mA cm⁻², 10 mA cm⁻², 12 mA cm⁻², 14 mA cm⁻² and 18 mA cm⁻², the degradation rate of the system was 32%, 57%, 67%, 76%, and 88% accordingly after 20 min of electrocatalytic reaction. The data showed that the increase in current density accelerated

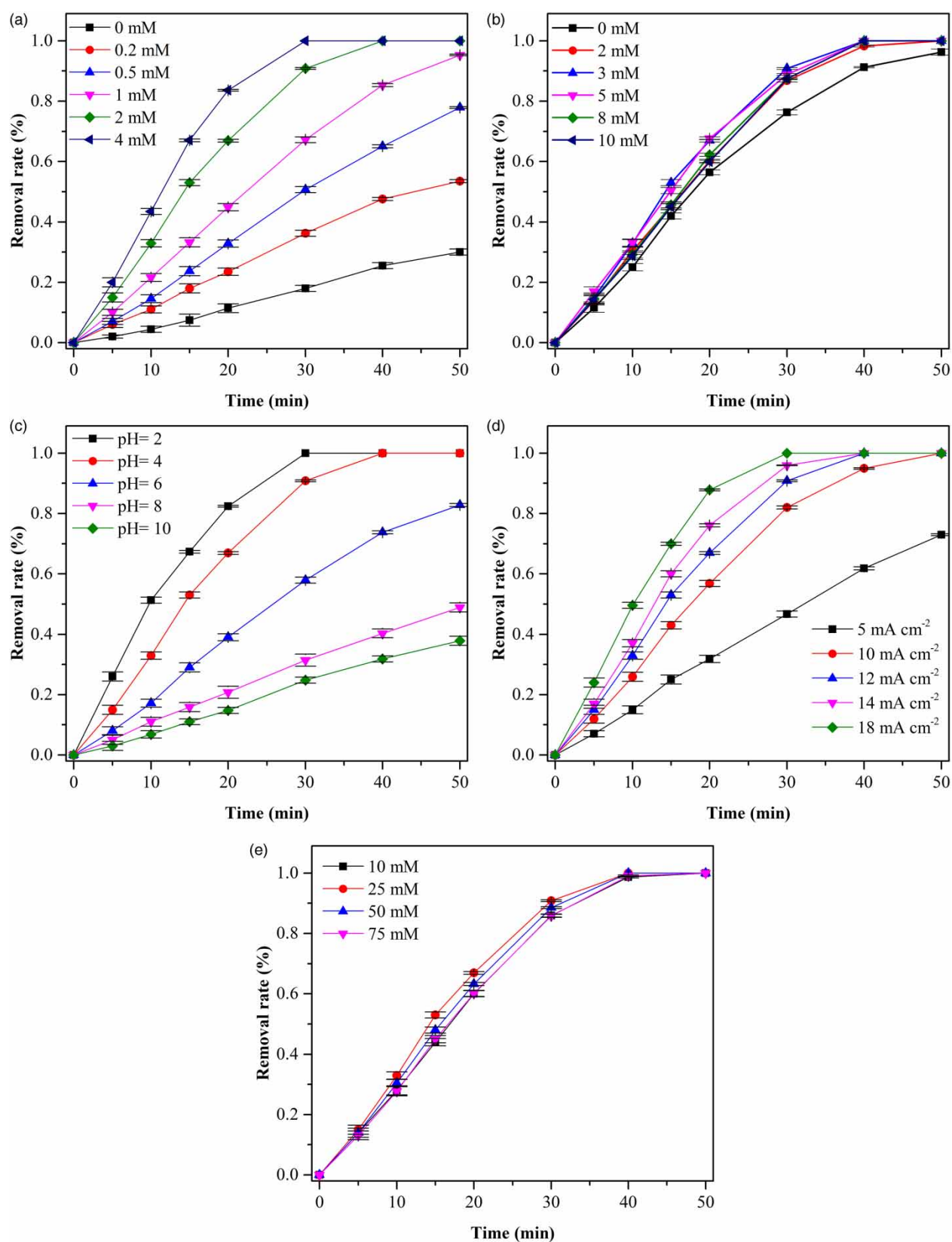


Figure 4 | Effect of (a) CO(II) concentration, (b) PO₄³⁻ concentration, (c) pH, (d) current density, (e) Na₂SO₄ concentration on MB removal (reaction conditions: initial MB concentration = 12.5 mg L⁻¹; initial pH = 4; current = 12 mA cm⁻²; stirring speed = 800 r min⁻¹; [Co(III)] = 2 mM; [PO₄³⁻] = 3 mM; [Na₂SO₄] = 25 mM).

the degradation of MB, and its current utilization rate showed a nonlinear decrease. This was because, as the current density increased, the following changes occurred in the system: first, the generation rate of Co(III) sped up, which improved the oxidation efficacy of the system; second, the direct electrocatalytic action of the electrode was enhanced; third, the side reactions (like the electrolysis of water) in the system was strengthened, which led to an increased energy consumption (see Table 1).

The increasing current density of the electrodes improved the degradation efficacy of the E-Co(II)-PO₄³⁻ system, and more energy was consumed accordingly. Considering the effects of energy consumption and degradation efficacy together, 12 mA cm⁻² was chosen to be the optimal current density in the E-Co(II)-PO₄³⁻ system.

Effect of Na₂SO₄ electrolyte

The electrolyte plays the role of electron transfer in the electrocatalytic system, and can be oxidized at the anode to generate various oxidation substances, which serves as a certain role of the mediated electrochemical oxidation (de Araujo *et al.* 2018). The degradation rate of the E-Co(II)-PO₄³⁻ system on MB at different concentrations of Na₂SO₄ electrolyte showed a rapid increase (the fastest condition was at 25 mM) within 30 min, and stabilized at a peak level (100%) at 50 min (the slowest condition was also at 25 mM). In a range of Na₂SO₄ concentration of 10 mM ~ 25 mM, the system voltage declined, the side reactions weakened, and the MB degradation rate rose with the increase in the Na₂SO₄ concentration; however, the amount of precipitates settling on the cathode surface increased, and the concentration of Co(III) and PO₄³⁻ in the solution reduced. At the same time, the proportion of PO₄³⁻ in the total amount of ions decreased with the increase in SO₄²⁻ concentration. Therefore, the contact rate of Co(III) and PO₄³⁻ with the anode went down, the yield of Co(III) and P₂O₈⁴⁻ dropped,

and thus the oxidation efficacy of the system reduced. Thus, on the basis of the two possible reasons mentioned above, the degradation efficacy of the E-Co(II)-PO₄³⁻ system on MB increased dramatically then slowly tended to become stable with the increase in the Na₂SO₄ concentration at a lower level (10 mM ~ 25 mM). Similarly, when the Na₂SO₄ concentration was higher (25 mM ~ 75 mM), the effect of the increase in the electrolyte concentration on the oxidation efficiency of the E-Co(II)-PO₄³⁻ system was inconspicuous.

Degradation mechanism of E-Co(II)-PO₄³⁻ system on MB

Analysis of intermediate products in MB degradation process

The intermediate products being generated in the MB degradation process (measured by liquid mass spectrometer, Q Exactive, China, 2018) are shown in Figure 5. Samples were taken at the degradation times of 10, 30 and 60 min (noted as sample 1, sample 2 and sample 3, respectively). When the retention time was 8.44 min, C₁₆H₁₈N₃S (m/z 284), C₁₆H₂₀N₃S (m/z 286), C₁₆H₁₈ON₃S (m/z 300) and C₁₆H₂₀ON₃S (m/z 302) were found in sample 1 and sample 2, and only a small amount of C₁₆H₂₀N₃S (m/z 286) occurred in sample 3; when the retention time was 7.40 min, C₁₅H₁₆N₃S (m/z 270) was detected in sample 1 and 2, which revealed that the electrocatalysis oxidation process of E-Co(II)-PO₄³⁻ system on MB and the intermediate degradation products was completed after 60 min of electrocatalysis. In addition, when the retention time was 1.82 min, C₈H₁₃N₂ (m/z 137) was detected in both samples 1 and 2, and C₁₂H₈NS (m/z 198) in sample 3 at the time of 14.58 min.

The possible degradation process of the E-Co(II)-PO₄³⁻ system on MB dye molecules is illustrated in Figure 6 based on the reports in the related research (Yu & Chuang 2007; Rauf *et al.* 2010; Alamo-Nole *et al.* 2013) and MB molecular structure. At first, the bond at the N-C junction of the MB molecule was broken (Yu & Chuang 2007; Rauf *et al.* 2010), which was mainly cracked from the branched dimethylamino group and the intermediate ring of phenothiazine, and intermediate substances were produced, such as phenothiazine, 2-amino-5-(N-methylformamide) benzene sulfonic acid and N₁,N₁-dimethyl-1,4 diaminobenzene (Alamo-Nole *et al.* 2013). Then the intermediates were degraded to aniline, phenol and benzene sulfonic acid, and eventually was decomposed into inorganic substances such as CO₂ and water.

Table 1 | Energy consumption on removing 50% MB at different current densities

Current density (mA cm ⁻²)	Voltage (V)	Time (min)	Energy consumption (J)
5	3.50	32	9.856
10	4.58	1.5	14.03
12	5.12	14	15.05
14	5.55	13	17.68
18	6.69	10	21.07

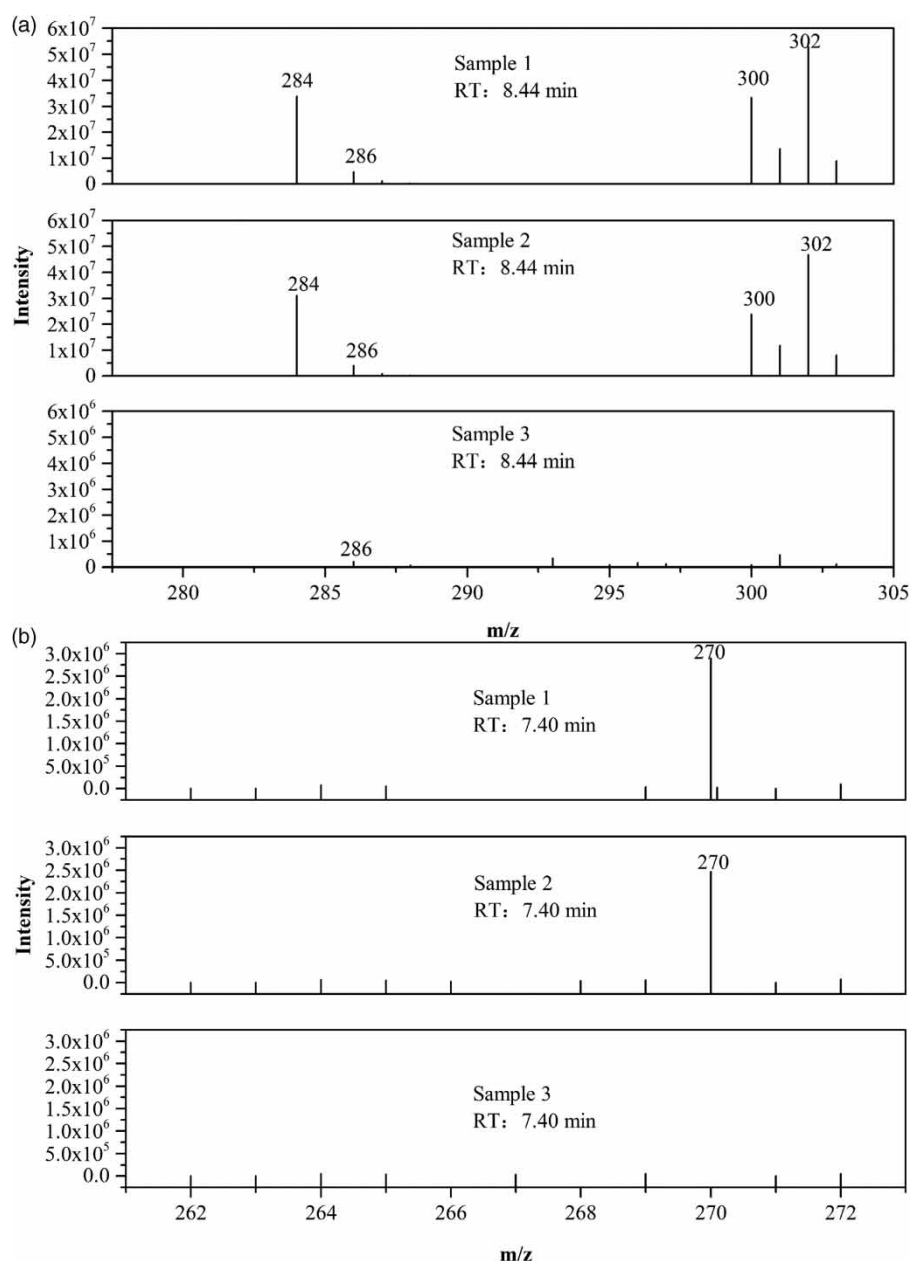


Figure 5 | The mass spectrometry analysis of MB degradation products.

Degradation mechanism of E-Co(II)- PO_4^{3-} system on MB

According to the analysis results and the types of intermediate oxidation products in the E-Co(II)- PO_4^{3-} electrocatalytic system, shown in the section *Types of Intermediate Oxidation Products in E-Co(II)- PO_4^{3-} System*, the possible degradation mechanism of the E-Co(II)- PO_4^{3-} system on MB is demonstrated in Figure 7.

From Figure 7, there were two types of electrocatalysis degradation mechanisms happening in the E-Co(II)- PO_4^{3-}

system. One was direct electrocatalytic action on platinum-titanium electrodes. Organic pollutants, Co(II) and PO_4^{3-} were anodized into the forms of small molecule organics, Co(III) and $\text{P}_2\text{O}_8^{4-}$, respectively. Another mechanism was indirect electrocatalysis of Co(III), $\text{P}_2\text{O}_8^{4-}$ and hydroxyl radicals generated in the electrocatalytic process. The electrocatalytic oxidation ability of Co(III) was dominant in the E-Co(II)- PO_4^{3-} system. On the one hand, organic matter (such as MB) in the solution was swiftly decomposed into small molecules (such as phenothiazine) because of the

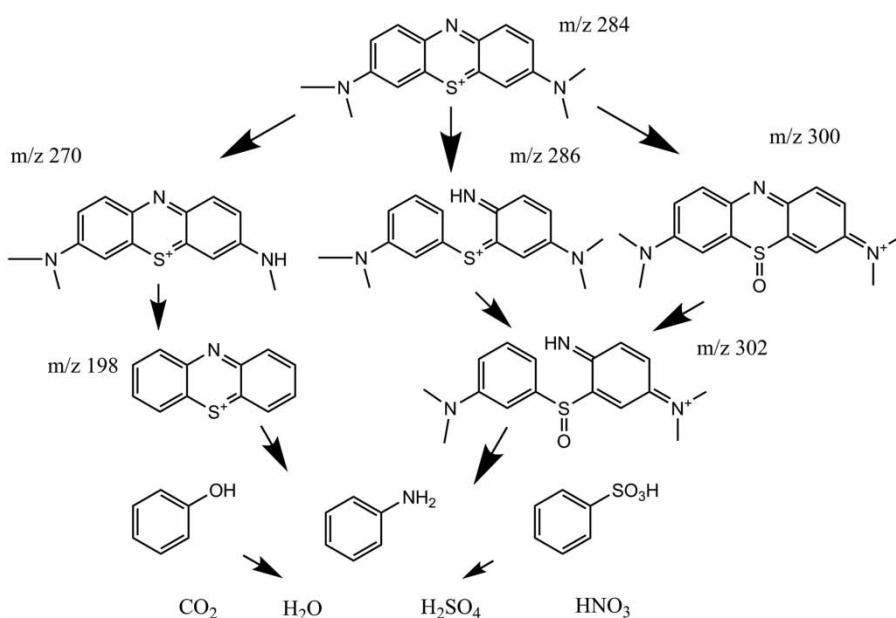


Figure 6 | The degradation schematic diagram of the E-Co(II)-PO₄³⁻ system on methylene blue (MB).

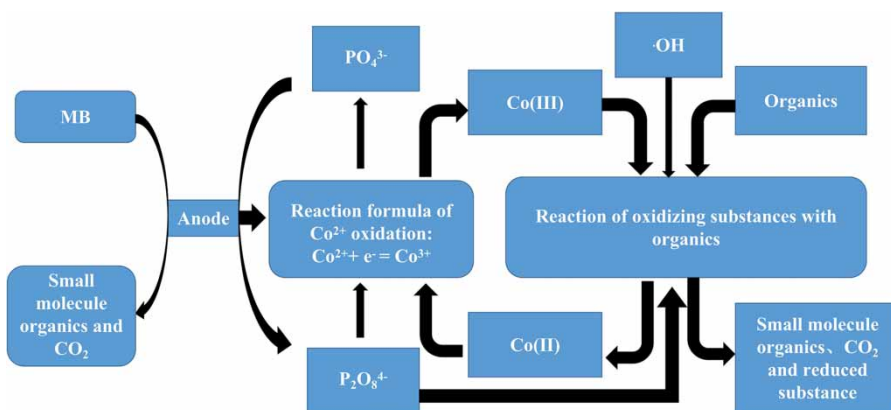


Figure 7 | Degradation mechanism diagram of E-Co(II)-PO₄³⁻ system on MB.

strong oxidation ability of Co(III). On the other hand, Co(III) was reduced to Co(II), thereby Co(II) can be recycled. At the same time, the P₂O₈⁴⁻ can oxidize organic matter (such as MB) and catalyze Co(II) to produce more Co(III), which further enhanced the oxidation ability of the system. The consumption of P₂O₈⁴⁻ promoted the reaction of PO₄³⁻ on the anode and produced more P₂O₈⁴⁻ to satisfy the chemical equilibrium. Therefore, the coupling system of PO₄³⁻ and E-Co(II) had a significant synergistic catalytic degradation efficacy on MB. In addition, a small number of hydroxyl radicals also oxidized the organic matter (such as MB) in the system (Figure 2(b)).

Therefore, there were two degradation mechanisms of the E-Co(II)-PO₄³⁻ system on MB; one was the direct electrocatalysis on the electrodes, and the other was the indirect oxidation of Co(III), P₂O₈⁴⁻, and hydroxyl radicals. Among them, the electrocatalytic oxidation of Co(III) was in dominion.

CONCLUSION

In this study, a novel synergistic electrocatalytic system (E-Co(II)-PO₄³⁻) was proposed and its degradation

performance was tested by adopting MB as a target pollutant. The removal rate of the E-Co(II)-PO₄³⁻ system on MB was as high as 100% in 40 min, which was 1.2 times that in E-Co(II) system and 5 times that in direct electrochemical oxidation. The TOC removal rate reached 60% in the E-Co(II)-PO₄³⁻ system, while that of the direct electrocatalytic system was only 23% correspondingly.

In the E-Co(II)-PO₄³⁻ system, the effect of the experimental factors on the MB removal rate was quite different. The three factors, like Co(II) concentration, current density and pH value had much stronger impact on degradation performance than these two, like the concentration of PO₄³⁻ and electrolyte.

The main intermediate active oxidation products in the E-Co(II)-PO₄³⁻ system were Co(III), accompanied with a small amount of hydroxyl radicals and P₂O₈⁴⁻. With direct electrocatalysis on the platinum titanium electrode and indirect oxidation of these intermediate oxidation products, MB was eventually degraded into inorganic substances like CO₂ and water. Among them, the electrocatalytic oxidation of Co(III) played a leading role.

ACKNOWLEDGEMENTS

The authors would like to thank the National Natural Science Foundation of China (No. 51378129 and 51108094), the Natural Science Foundation of Guangdong Province (No. 2015A030313494 and 2017A030313321) and the Higher Education Department of Guangdong province characteristic innovation project of colleges and Universities (No. 2016KTSCX035) for their financial support.

DATA AVAILABILITY STATEMENT

All relevant data are included in the paper or its Supplementary Information.

REFERENCES

- Alamo-Nole, L., Bailon-Ruiz, S., Luna-Pineda, T., Perales-Perez, O. & Roman, F. R. 2013 Photocatalytic activity of quantum dot-magnetite nanocomposites to degrade organic dyes in the aqueous phase. *Journal of Materials Chemistry A* **1** (18), 5509–5516. <https://doi.org/10.1039/c3ta01135f>.
- Brillas, E. 2020 A review on the photoelectro-Fenton process as efficient electrochemical advanced oxidation for wastewater remediation. Treatment with UV light, sunlight, and coupling with conventional and other photo-assisted advanced technologies. *Chemosphere* **250**, 126198. <https://doi.org/10.1016/j.chemosphere.2020.126198>.
- Chaplin, B. P. 2014 Critical review of electrochemical advanced oxidation processes for water treatment applications. *Environ Sci Process Impacts* **16** (6), 1182–1203. <https://doi.org/10.1039/c3em00679d>.
- Chung, Y. H. & Park, S. M. 2000 Destruction of aniline by mediated electrochemical oxidation with Ce(IV) and Co(III) as mediators. *Journal of Applied Electrochemistry* **30** (6), 685–691.
- Costa, C. R., Montilla, F., Morallón, E. & Olivi, P. 2009 Electrochemical oxidation of acid black 210 dye on the boron-doped diamond electrode in the presence of phosphate ions: effect of current density, pH, and chloride ions. *Electrochimica Acta* **54** (27), 7048–7055. <https://doi.org/10.1016/j.electacta.2009.07.027>.
- Cui, H. J., Huang, H. Z., Yuan, B. & Fu, M. L. 2015 Decolorization of RhB dye by manganese oxides: effect of crystal type and solution pH. *Geochemical Transactions* **16**, 10. <https://doi.org/10.1186/s12932-015-0024-2>.
- Dassanayake, R. S., Rajakaruna, E. & Abidi, N. 2018 Preparation of aeroclitin-TiO₂ composite for efficient photocatalytic degradation of methylene blue. *Journal of Applied Polymer Science* **135** (8), 45908. <https://doi.org/10.1002/app.45908>.
- de Araujo, D. M., Saez, C., Canizares, P., Rodrigo, M. A. & Martinez-Huitle, C. A. 2018 Improving the catalytic effect of peroxodisulfate and peroxodiphosphate electrochemically generated at diamond electrode by activation with light irradiation. *Chemosphere* **207**, 774–780. <https://doi.org/10.1016/j.chemosphere.2018.05.121>.
- Dhall, P., Kumar, R. & Kumar, A. 2012 Biodegradation of sewage wastewater using autochthonous bacteria. *Scientific World Journal* **2012**, 861–903. <https://doi.org/10.1100/2012/861903>.
- Doltabadi, M., Alidadi, H. & Davoudi, M. 2016 Comparative study of cationic and anionic dye removal from aqueous solutions using sawdust-based adsorbent. *Environmental Progress & Sustainable Energy* **35** (4), 1078–1090. <https://doi.org/10.1002/ep.12334>.
- Elnakar, H. & Buchanan, I. 2020 Treatment of bypass wastewater using novel integrated potassium ferrate(VI) and iron electrocoagulation system. *Journal of Environmental Engineering* **146** (8), 04020075. [https://doi.org/10.1061/\(ASCE\)EE.1943-7870.0001754](https://doi.org/10.1061/(ASCE)EE.1943-7870.0001754).
- Ghanbarlou, H., Nasernejad, B., Nikbakht Fini, M., Simonsen, M. E. & Muff, J. 2020 Synthesis of an iron-graphene based particle electrode for pesticide removal in three-dimensional heterogeneous electro-Fenton water treatment system. *Chemical Engineering Journal* **395**. <https://doi.org/10.1016/j.cej.2020.125025>.
- Govindan, M. & Moon, I. S. 2013 A single catalyst of aqueous Co(III) for deodorization of mixture odor gases: a development and reaction pathway study at electro-scrubbing

- process. *Journal of Hazardous Materials* **260**, 1064–1072. <https://doi.org/10.1016/j.jhazmat.2013.06.055>.
- Hariharan, S. S. & Maruthamuthu, M. 1979 Polymerization of acrylonitrile initiated by the redox-system peroxodiphosphate-co(II). *Macromolecular Chemistry & Physics* **180** (10), 2513–2515.
- Liu, Z., Zhao, C., Wang, P., Zheng, H., Sun, Y. & Dionysiou, D. D. 2018 Removal of carbamazepine in water by electro-activated carbon fiber-peroxydisulfate: comparison, optimization, recycle, and mechanism study. *Chemical Engineering Journal* **343**, 28–36. <https://doi.org/10.1016/j.cej.2018.02.114>.
- Lubis, R. A., Bahti, H. H., Hastiawan, I. & Mulcahy, D. 2015 Optimization in mediated electrochemical oxidation using cobalt sulfate as a mediator. *Procedia Chemistry* **17**, 153–156. <https://doi.org/10.1016/j.proche.2015.12.103>.
- Nidheesh, P. V., Zhou, M. & Oturan, M. A. 2018 An overview on the removal of synthetic dyes from water by electrochemical advanced oxidation processes. *Chemosphere* **197**, 210–227. <https://doi.org/10.1016/j.chemosphere.2017.12.195>.
- Okubo, T., Yamamura, Y. & Ise, N. 2010 Role of solvation and desolvation in polymer 'Catalysis' [1]. VI. influence of ionic valencies of reactants on the desolvation effects in the spontaneous and Hg^{2+} -induced aquation of $\text{Co}(\text{NH}_3)_5\text{SO}_4^+$, $\text{Co}(\text{NH}_3)_5\text{br}^{2+}$ and $\text{Cr}(\text{NH}_3)_5\text{br}^{2+}$. *Zeitschrift für Elektrochemie Berichte Der Bunsengesellschaft für Physikalische Chemie* **86** (10), 922–925.
- Rauf, M. A., Meetani, M. A., Khaleel, A. & Ahmed, A. 2010 Photocatalytic degradation of Methylene Blue using a mixed catalyst and product analysis by LC/MS. *Chemical Engineering Journal* **157** (2–3), 373–378. <https://doi.org/10.1016/j.cej.2009.11.017>.
- Sekar, S., Surianarayanan, M., Ranganathan, V., MacFarlane, D. R. & Mandal, A. B. 2012 Choline-based ionic liquids-enhanced biodegradation of azo dyes. *Environmental Science & Technology* **46** (9), 4902–4908. <https://doi.org/10.1021/es204489h>.
- Soleymani, A. R. & Moradi, M. 2018 Performance and modeling of UV/persulfate/Ce(IV) process as a dual oxidant photochemical treatment system: kinetic study and operating cost estimation. *Chemical Engineering Journal* **347**, 243–251. <https://doi.org/10.1016/j.cej.2018.04.093>.
- Wang, Q., Jin, T., Hu, Z., Zhou, L. & Zhou, M. 2013 TiO_2 -NTs/ SnO_2 -Sb anode for efficient electrocatalytic degradation of organic pollutants: effect of TiO_2 -NTs architecture. *Separation and Purification Technology* **102**, 180–186. <https://doi.org/10.1016/j.seppur.2012.10.006>.
- Wang, S., Wang, J., Wang, T., Li, C. & Wu, Z. 2019 Effects of ozone treatment on pesticide residues in food: a review. *International Journal of Food Science & Technology* **54** (2), 301–312. <https://doi.org/10.1111/ijfs.13938>.
- Yi, S.-C., Jung, C. Y. & Kim, W. J. 2011 Synthesis of Pt/PEI-MWCNT composite materials on polyethyleneimine-functionalized MWNTs as supports. *Materials Research Bulletin* **46** (12), 2433–2440. <https://doi.org/10.1016/j.materresbull.2011.08.025>.
- Yu, Z. & Chuang, S. S. 2007 Probing methylene blue photocatalytic degradation by adsorbed ethanol with in situ IR. *The Journal of Physical Chemistry C* **111** (37), 13813–13820.

First received 5 November 2020; accepted in revised form 4 January 2021. Available online 12 January 2021